

# Mixing small proteins with lipids and cholesterol

Subhadip Basu<sup>1</sup> and Oded Farago<sup>1</sup>

*Department of Biomedical Engineering, Ben Gurion University of the Negev  
Be'er Sheva 84105, Israel*

(\*Electronic mail: ofarago@bgu.ac.il)

(Dated: 26 November 2024)

Many ternary mixtures composed of saturated and unsaturated lipids with cholesterol (Chol) exhibit a region of coexistence between liquid-disordered ( $L_d$ ) and liquid-ordered ( $L_o$ ) domains, bearing some similarities to lipid rafts in biological membranes. However, biological rafts also contain many proteins that interact with the lipids and modify the distribution of lipids. Here, we extend a previously published lattice model of ternary DPPC/DOPC/Chol mixtures by introducing a small amount of small proteins (peptides). We use Monte Carlo simulations to explore the mixing phase behavior of the components as a function of the interaction parameter representing the affinity between the proteins and the saturated DPPC chains, and for different mixture compositions. At moderate fractions of DPPC, the system is in a two-phase  $L_d + L_o$  coexistence, and the proteins exhibit a simple partition behavior between the phases that depends on the protein-lipid affinity parameter. At low DPPC compositions, the mixture is in  $L_d$  phase with local nanoscopic ordered domains. Addition of proteins with sufficiently strong attraction to the saturated lipids can induce the separation of a distinct  $L_o$  large domain with tightly-packed gel-like clusters of proteins and saturated lipids. Consistent with the theory of phase transitions, we observe that the domain sizes grow when the mixture composition is in the vicinity of the critical point. Our simulations show that the addition of a small amount of proteins to such mixtures can cause their size to grow even further, and lead to the formation of metastable dynamic  $L_o$  domains with sizes comparable to biological rafts.

## I. INTRODUCTION

Cell membranes are thin bilayer sheets that define the boundaries of cells and their internal organelles. In addition to protecting the cells, membranes also play important roles in various cellular functions like signal transduction, molecular transports, and molecular organization of cellular processes.<sup>1,2</sup> Composition wise, biological membranes consist of hundreds of different types of lipids<sup>3,4</sup>, which can be divided into three main categories: phospholipids, glycolipids and sterols.<sup>1,2,5</sup> While the lipids constitute the main element of the cell membrane, about 50% of the area of the membrane is occupied by proteins.<sup>1,6</sup> Many of the membrane functions like cell-to cell communication and active transport of molecules are associated with these proteins.<sup>7-9</sup>

Lateral organization of lipids in the membrane leaflets and its correlation to the membrane functionalities has been a topic of scientific interest for several decades. Back in 1972, the fluid-mosaic model was proposed, describing the cell membranes as a random mixture of lipids with proteins embedded within.<sup>10</sup> Soon later, it was realized experimentally<sup>11-13</sup> that although entropy favors random mixing, interactions between different types of lipids may promote the formation of membrane domains with different lipid compositions.<sup>2,14,15</sup> This has led to the development of the lipid raft hypothesis:<sup>16</sup> Rafts are defined as heterogeneous, dynamic, cholesterol and sphingolipid-enriched membrane domains (10-200 nm), with a potential to form microscopic domains (> 300nm) in presence of proteins.<sup>17</sup> Rafts are liquid-ordered ( $L_o$ ) domains, having properties intermediate between the liquid-disordered ( $L_d$ ) and gel ( $S_o$ ) phases.<sup>18</sup> Similarly to the former, the lipids in the liquid-ordered domains are mobile and free to diffuse in the membrane plane.<sup>19</sup> However, their hydrocarbon chains are ordered, fully extended and tightly packed, as in the gel phase.<sup>20</sup>

One of the potential routes to investigate the lateral arrangement of lipids in the cell membrane is to map out its phase diagram. Unfortunately, the structural complexity of real biological membranes makes such a task almost impossible. Therefore, efforts have been made to establish the phase diagram of compositionally simpler model systems, especially of ternary lipid mixtures composed of a unsaturated low melting temperature lipid (like DOPC), a saturated high melting temperature lipid (like DPPC) and cholesterol (Chol).<sup>21</sup> Investigations of many such ternary mixtures revealed regions of phase coexistence between the  $L_o$  phase, dominated by saturated lipids and Chol population, and a  $L_d$  phase, composed mainly of unsaturated lipids.<sup>22-25</sup> Depending on the identity of the lipids and temperature, the liquid-liquid phase separation may be macroscopic-thermodynamic (Type II mixtures) or local (Type I mixtures).<sup>22</sup> The latter case seems to be more relevant to lipid rafts in complex biological membranes which, as noted above, are of typical size of several tens of nanometers. At high fractions of the saturated lipids, the phase diagrams of ternary mixtures also include regions of coexistence between the liquid phases and the gel  $S_o$  phase, where the saturated lipids are immobile and very tightly packed.

Several experimental techniques like fluorescence microscopy,<sup>26-28</sup> Förster Resonance Energy Transfer (FRET),<sup>29-32</sup> Interferometric Scattering Microscopy,<sup>33,34</sup> Atomic Force Microscopy (AFM),<sup>35,36</sup> Nuclear Magnetic Resonance (NMR)<sup>24,37</sup> have been successfully applied to detect lipid domains. Apart from experimental means, Molecular Dynamics (MD) and Monte Carlo (MC) simulations have been extensively used to investigate lipid domain formation.<sup>38-40</sup> All-atom MD simulations revealed many structural details of lipid domains like the presence of sub-structures within them.<sup>41-43</sup> The role of sterols in packing of lipids have also been investigated using all-atom

MD simulation.<sup>44</sup> However, because of the large temporal and spatial scales associated with the process, most atomistic simulations of lipid mixtures capture only the onset of the formation of liquid ordered domains.<sup>39,45–47</sup> To access larger length- and time-scales, coarse-grained (CG) simulations have been employed to observe phase separation,<sup>48–52</sup> and the phase diagrams of different ternary lipid mixtures have been determined and found to be in good agreement with experimental findings.<sup>53–57</sup> Besides atomistic and CG simulations of specific mixtures, ultra CG and lattice models have been also developed to probe phase separation phenomena in lipid mixtures.<sup>58–61</sup> Such models facilitate simulations of complete phase separation in very large systems, and their simplicity can help characterizing the mechanisms governing the thermodynamic behavior of lipid-Chol mixtures.

Proteins may show affinity to specific lipid domains which has implications in many cellular phenomena. Certain glycosylphosphatidylinositol (GPI)-anchored proteins are associated with lipid rafts.<sup>62</sup> B-cell receptor (BCR) proteins tend to aggregate in the  $L_o$  domains, and such preferential localization was reported to facilitate BCR activation.<sup>63</sup> Segregation property of another similar protein, namely T-cell receptors (TCR), remain controversial, as its affinity toward both  $L_o$  and  $L_d$  domains has been reported.<sup>64,65</sup> Protein partitioning in the neuronal membrane is also of significant importance. There are reports on the raft-dependent functionality of neurotransmitters like choline and serotonin.<sup>66,67</sup> Some nerve growth factors, like *trkA* and *p75*, also prefer to reside and cluster in the  $L_o$  domain in their bound states.<sup>68,69</sup> Moreover,  $L_o$  domains also promote the formation of amyloid- $\beta$  and fibril aggregation, associated with the development of Alzheimer's disease.<sup>69–71</sup> Viral assembly sites of HIV are generally located in the ordered domains of the lipid membrane because of the affinity of *gag* protein, a significant player in the viral assembly process, toward cholesterol and sphingolipid.<sup>72</sup> On the other hand, the fusion peptide (FP) of HIV gp41 envelop protein exhibits no specific preference to either ordered or disordered domains.<sup>73,74</sup>

The partition of peptides and proteins between membrane domains has been also studied via computer simulations. For example, model peptides, KALP and WALP, prefer to partition to the  $L_d$  phase, because of the lower free energy in the disordered region.<sup>75,76</sup> Similar partitioning preference toward  $L_d$  regions was noted for rhodopsin, a G-protein coupled receptor, and 7-TM protein bacteriorhodopsin.<sup>40,77,78</sup> CG simulations demonstrated that H-Ras proteins accumulate at  $L_d - L_o$  interfaces, while Hedgehog proteins prefer the  $L_o$  domains.<sup>79,80</sup>

The affinity of proteins to different phases of lipid membranes depends on many factors. Proteins with longer hydrophobic transmembrane domain (TMD) tend to reside in the thicker liquid ordered phase because of hydrophobic mismatch considerations.<sup>81–83</sup> On the other hand, proteins that have TMD with a larger accessible surface area, exhibit lesser affinity to the  $L_o$  phase.<sup>69,84</sup> Chemical modifications can change the affinity of proteins. For example, HIV gp160, and N-RAS proteins exhibit affinity to ordered domains after palmitoylation, whereas the distribution of palmitoylated

tLAT remains controversial.<sup>82,85</sup>

Proteins are not only attracted to different liquid phases of heterogeneous lipid membranes, but also influence the phase behavior itself. Some proteins like lectins can bind to carbohydrates/glycols attached to lipids, leading to heterogeneous lateral organization of lipids.<sup>86</sup> BCRs are known to control the size and stability of liquid ordered domains.<sup>63</sup> Specific and non-specific interactions between TMDs of integral proteins and lipids<sup>87–89</sup> and hydrophobic mismatch<sup>90</sup> may also promote formation of lipid domains. It is worth reminding here that another protein component of the cell cortex, namely actin, which is also believed to contribute to lipid raft formation.<sup>91</sup> In general, the mechanisms by which proteins influence the heterogeneity of the lipid membranes are far from clear.<sup>92–94</sup>

The present study aims to extend the previously developed minimal lattice model of ternary mixtures of saturated and unsaturated lipids with Chol.<sup>58,59,95</sup> Here, we add to the model a small fraction of objects representing small proteins (peptides), and examine their partition between the liquid-disordered and liquid-ordered regions, and their influence on the phase behavior of the mixture. As before, the model involves only nearest-neighbor interactions. We keep the number of interaction parameters minimal by assuming that the proteins have no direct interactions between themselves, and considering only interactions between the peptides and the saturated ordered chains. We analyze the partition of the model proteins between the liquid phases, and explore their influence on the formation, stability, and characteristics of the liquid-ordered domains.

## II. METHODS

The lattice model introduced herein is an extension of a previous model of ternary mixtures consisting of saturated (DPPC) and unsaturated (DOPC) lipids with Chol<sup>58,59</sup>. As in previous studies, the simulations are conducted on a triangular lattice of  $121 \times 140 = 16940$  sites with periodic boundary conditions and lattice spacing  $l \simeq 0.56$  nm. This value of  $l$  is set to match area density of DPPC in the liquid-ordered state (see details in ref. 58). The lipids are modeled as dimers with their two acyl chains occupying adjacent lattice sites, and Chol is modeled as a monomer. Into this mixture, we now introduce small proteins (peptides) that are represented as triangle-shaped trimers.

To sample the phase space of the system, we perform MC simulations involving displacement of monomers, rotation of dimers (displacement of one chain), and flips of trimers (reflection of one vertex across the edge connecting the other two). Some lattice sites are left empty to allow molecular diffusion within the system. Moves are accepted by the Metropolis criterion, and only if the displaced particle lands on a vacant site or a site occupied by a Chol monomer, in which case the Chol swaps places with the displaced particle. The DOPC unsaturated chains are disordered, while the DPPC saturated chains may be either ordered or disordered. Therefore, the simulations also include attempts to change the

state of such chains. We define a MC time unit as a collection of  $1.05 \times 10^8$  trial moves, of which 95% are displacements/rotations/reflections of particles, and the rest 5% are attempts to change the state (ordered/disordered) of randomly chosen DPPC chains. The length of the simulations extends between 1000 to 16000 time units, depending on the composition and the phase behavior. Properties of interest have been calculated only after the system equilibrated from the initial random configuration and the energy saturated to the equilibrium value. For each simulated mixture, we have performed independent runs with different initial configurations to verify the consistency of the equilibrated states.

To summarize, each lattice site can be assigned one of the following six states: (i) void ( $s = 0$ ), (ii) disordered DPPC ( $s = 1$ ), (iii) ordered DPPC ( $s = 2$ ), (iv) Chol ( $s = 3$ ), (v) DOPC ( $s = 4$ ), and (vi) protein ( $s = 5$ ). In the model, the molecular forces are represented by nearest-neighbor interactions only. Explicitly, the model Hamiltonian reads:

$$\begin{aligned}
 E = & -\Omega k_B T \sum_i \delta_{s_i,1} - \sum_{i,j} \epsilon_{22} \delta_{s_i,2} \delta_{s_j,2} \\
 & - \sum_{i,j} \epsilon_{23} [\delta_{s_i,2} \delta_{s_j,3} + \delta_{s_i,3} \delta_{s_j,2}] \\
 & - \sum_{i,j} \epsilon_{24} [\delta_{s_i,2} \delta_{s_j,4} + \delta_{s_i,4} \delta_{s_j,2}] \\
 & - \sum_{i,j} \epsilon_{25} [\delta_{s_i,2} \delta_{s_j,5} + \delta_{s_i,5} \delta_{s_j,2}] \\
 & - \sum_{i,j} \epsilon_{55} \delta_{s_i,5} \delta_{s_j,5},
 \end{aligned} \tag{1}$$

where the sums run over all pairs of nearest neighbor sites ( $i, j$ ), except for the first term, where the summation is over all the lattice sites. This term accounts for the entropy gained when a DPPC chain is in disordered ( $s = 1$ ), relative to the ordered ( $s = 2$ ) state. The other terms in Eq. (1) correspond, in order of appearance, to the short-range attraction between an ordered DPPC chain with another ordered DPPC chain, Chol, a disordered DOPC chain, and a peptide. The last term represents protein-protein interactions. We use the same model parameters as in our previous studies:  $\Omega = 3.9$ ,  $\epsilon_{22} = 1.3\epsilon$ ,  $\epsilon_{23} = 0.72\epsilon$ . These values were set in the simulations of binary DPPC/Chol mixtures<sup>58</sup> to reproduce the phase diagram of such mixtures as a function of the Chol mole fraction, at temperatures near the melting temperature of pure DPPC membranes  $T_m = 314K = 0.9/k_B\epsilon$ . In the following study where DOPC lipids were added to the system<sup>59</sup>, we found that further setting  $\epsilon_{24} = 0$  yields results that agrees very well with the experimentally-established phase diagram of DPPC/DOPC/Chol mixtures at temperatures in the range between 280 and 300 degrees Kelvin.<sup>24,37,96,97</sup> The phase diagram of the mixture is plotted in fig. 1(a). Importantly, it includes a two-phase region of coexistence between the liquid-ordered and liquid-disordered phases which is marked by the grey-shaded area. DPPC/DOPC/Chol is known as a ‘‘Type II’’ mixture, i.e., a mixture where the two liquid phases are macroscopically (thermodynamically) separated.

In this paper, we study the influence of a small density of peptides on the phase diagram of the ternary mixture. For this

purpose, we include 100 peptide trimers in the mixture (covering 2% of the lattice area), and simulate the system at different lipid-Chol compositions corresponding to different regions of the phase space. Our aim here is *not* to investigate specific peptides, but to explore to possible impact of adding peptides to the DPPC/DOPC/Chol mixture. Since the peptide-DPPC attraction competes with the DPPC-DPPC attraction (which is the driving the formation of ordered domains), we chose to vary  $\epsilon_{25}$  between 0 and  $2\epsilon_{22} = 2.6\epsilon$  which, as will be shown below, covers a spectrum of distinct phase behaviors. We also set  $\epsilon_{55} = 0$  and so the proteins in the present study are assumed to be non-interacting.

In the following section, we show many equilibrium snapshots of mixtures at different compositions and for different values of the model parameter  $\epsilon_{25}$ . In these snapshots, the system is divided into liquid-disordered ( $L_d$ ), liquid-ordered ( $L_o$ ), and gel ( $S_o$ ) regions, which are displayed in purple, yellow, and black, respectively. The division of the system between the different regions is based on the simple algorithm introduced in our previous simulation study of ternary mixtures, which has been modified here to account for the presence of proteins. In the original algorithm (see full details in ref. 59), we assign each state of the lattice sites with the following orderliness score,  $S_i$ : A void, ordered DPPC chain, disordered DPPC chain, Chol, and DOPC chain, gets a score of 0, 2, -0.5, 1, and -1, respectively. The order parameter,  $G_i$ , of a lattice site is given by

$$G_i = S c_i + W_i \sum_{j=1}^6 S c_j, \tag{2}$$

where the sum runs over the six nearest-neighbor sites. In ternary mixture simulations without proteins, we set  $W_i = 1$ . In the present study, a site with a protein gets a zero score, and  $W_i = 6/(6 - N_i^p)$ , where  $0 \leq N_i^p < 6$  is the number of nearest-neighbor sites occupied by proteins. If all the neighbors are occupied by proteins ( $N_i^p = 6$ , a scenario that actually never encountered in the simulations), then we simply set  $G_i = S c_i$ . Sites with negative (non-negative) grades,  $G_i < 0$  ( $G_i \geq 0$ ) are associated with the liquid-disordered (liquid-ordered) regions. The site with the maximum possible order parameter,  $G_i = 14$ , constitute the gel region. The sites hosting the proteins are plotted in green irrespective of their grade.

Some properties of the larger ordered domains have been computed. The Hoshen–Kopelman algorithm<sup>98</sup>, adopted for a periodic triangular lattice, has been used to identify these domains, and their radius of gyration was also calculated

$$R_g = \sqrt{\frac{1}{2N^2} \sum_{i \neq j} |r_i - r_j|^2}, \tag{3}$$

where the sum is carried over all the pairs of points belonging to a domain.

### III. RESULTS AND DISCUSSION

Our goal is to study how the addition of a small fraction of peptides modifies the lateral organization and phase be-

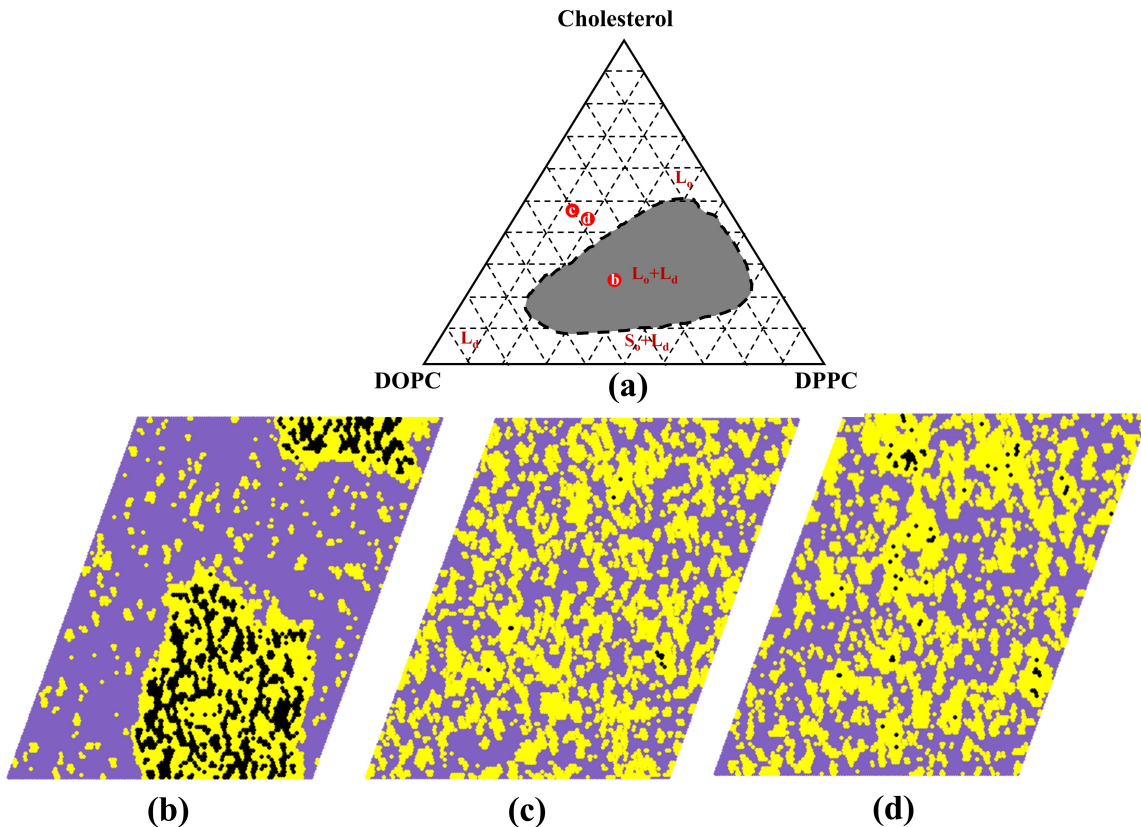


FIG. 1. (a) The phase diagram of a ternary DPPC/DOPC/Chol mixture at  $T = 298K$ , adapted from ref. 37. The grey shaded area is the region of liquid-liquid phase coexistence. The red dots indicate the compositions of the simulated systems, whose equilibrium snapshots are shown in (b)-(d), respectively. The liquid-disordered ( $L_d$ ), liquid-ordered ( $L_o$ ), and gel ( $S_o$ ) sites are colored in purple, yellow, and black, respectively. The compositions of the simulated systems are given in Table I.

TABLE I. Compositions of ternary lipid mixtures simulated in this work. The roman alphabets within the brackets in the first column indicates the corresponding snapshot in Fig. 1

Designation	DPPC (mol%)	DOPC (mol%)	Chol (mol%)
35DPPC (b)	35	40	25
12DPPC (c)	12	40	48
18DPPC (d)	18	38	44

havior of ternary mixtures of saturated DPPC and unsaturated DOPC lipids with Chol. For this purpose, we add 100 trimers representing small peptides to mixtures with lipid compositions given in Table I. In this table, point (b) corresponds to a mixture exhibiting macroscopic  $L_d + L_o$  coexistence. The other two compositions [(c) and (d)] correspond to the one-phase region where the system is homogeneous on macroscopic scales, and features local density fluctuations appearing as small nanoscopic ordered regions in a liquid-disordered background. Point (d) is close to a miscibility transition point, as evident from the larger size of the ordered domains and the fact that the system is on the verge of percolation.

#### A. Protein partitioning in the two-phase regime

We start with the simpler case of the two-phase regime. As discussed earlier, different biological processes involve protein accumulations in either the liquid-disordered or liquid-ordered regions. This feature is easily captured in our simulations, as illustrated in fig. 2, showing how the affinity of the proteins to the two phases varies as a function of the interaction parameter  $\epsilon_{25}$ . The snapshots in the figure show equilibrium distributions for 35DPPC [point (b), in fig. 1], corresponding to (a)  $\epsilon_{25} = 0$ , (b)  $0.75\epsilon$ , and (c)  $1.95\epsilon$ . The trend in these snapshots is clear. The  $L_o$  phase is stabilized by the short-range packing attraction of the saturated ordered lipids to the Chol molecules ( $\epsilon_{23}$ ) and, especially, to each other ( $\epsilon_{22}$ ).

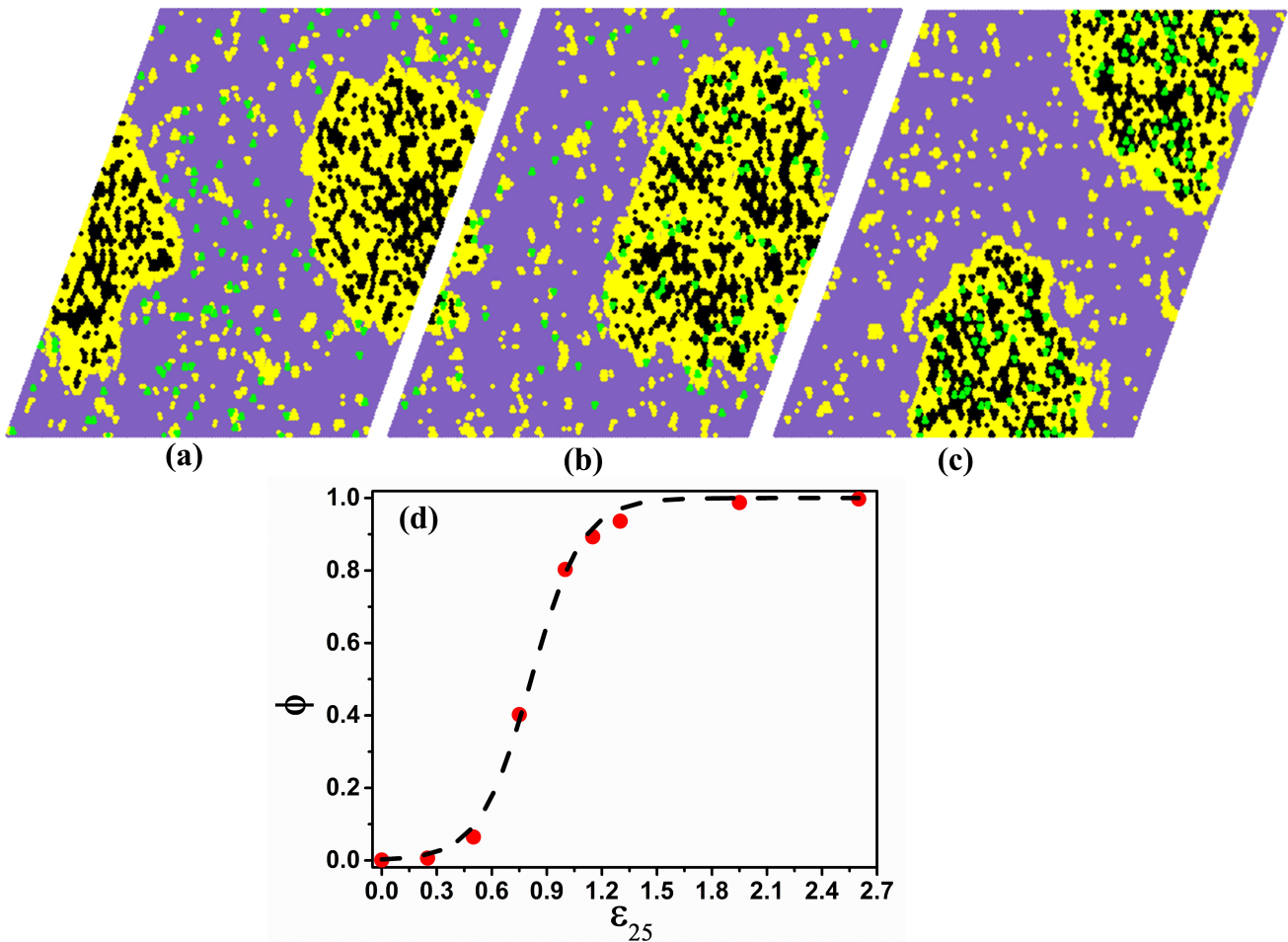


FIG. 2. Partitioning of proteins in the two phase region (35DPPC) of DPPC/DOPC/Chol mixture for varying strength of  $\epsilon_{25}$ . Snapshots (a), (b), and (c) show equilibrium distributions of systems corresponding to  $\epsilon_{25} = 0$ ,  $0.75\epsilon$ , and  $1.95\epsilon$ , respectively. Color coding the same as in fig. 1, with proteins marked by green. (d) The fraction,  $0 \leq \phi \leq 1$  of the proteins completely inside the  $L_o$  phase, as a function of  $\epsilon_{25}$ . The dashed line is a fit of the results to Eq. (4) with  $a \simeq 7.2$  and  $b \simeq 5.8$ .

Therefore, insertion of proteins into the liquid-ordered phase depends on the competition between these packing interactions and the attraction of the proteins to the ordered chain ( $\epsilon_{25}$ ). Accordingly, we see in fig. 2 that proteins are completely expelled from the  $L_o$  phase for  $\epsilon_{25} = 0$  (a), partially penetrate the ordered region for  $\epsilon_{25} = 0.75\epsilon$  (b), and become fully encapsulated in it for  $\epsilon_{25} = 1.95\epsilon$  (c).

A quantitative representation of the protein partitioning between the liquid-disordered and liquid-ordered for 35DPPC mixture is found in Fig. 2(d), where the fraction,  $0 \leq \phi \leq 1$  of the proteins completely inside the  $L_o$  phase (protein trimers having all of their 9 neighbors from the  $L_o$  phase) is plotted as a function of  $\epsilon_{25}$ . The graph shows a sharp crossover in the distribution of the proteins between the two phases. The change in the protein distribution can be related to the difference in the solvation free energy,  $\Delta F$ , of the small proteins in the two liquid phases. It is reasonable to assume that  $\Delta F = -a\epsilon_{25} + b$ , where the first term represents the attraction between the proteins and the ordered DPPC chains, with  $a \leq 12$  being the average number of nearest neighbors inter-

actions, per protein, with ordered DPPC chains. The second term accounts for all the other thermodynamic considerations, including the competing lipid-lipid and lipid-Chol interactions in the  $L_o$  phase, as well as the contribution due to mixing entropy. At a small density of proteins, collective effects in the partitioning behavior may be neglected, and we can expect that

$$\phi = \frac{\exp[(a\epsilon_{25} - b)/k_B T]}{1 + \exp[(a\epsilon_{25} - b)/k_B T]} \quad (4)$$

The dashed curve in fig. 2(d) is a fit of the results to Eq. (4) with  $a \simeq 7.2$  and  $b \simeq 5.8$ .

## B. Formation of large domains in the one-phase region

The influence of small proteins on mixtures in the one-phase region is more interesting than in the two phase region. The one-phase region is locally inhomogeneous, featuring nanoscopic ordered domains. Addition of even a small

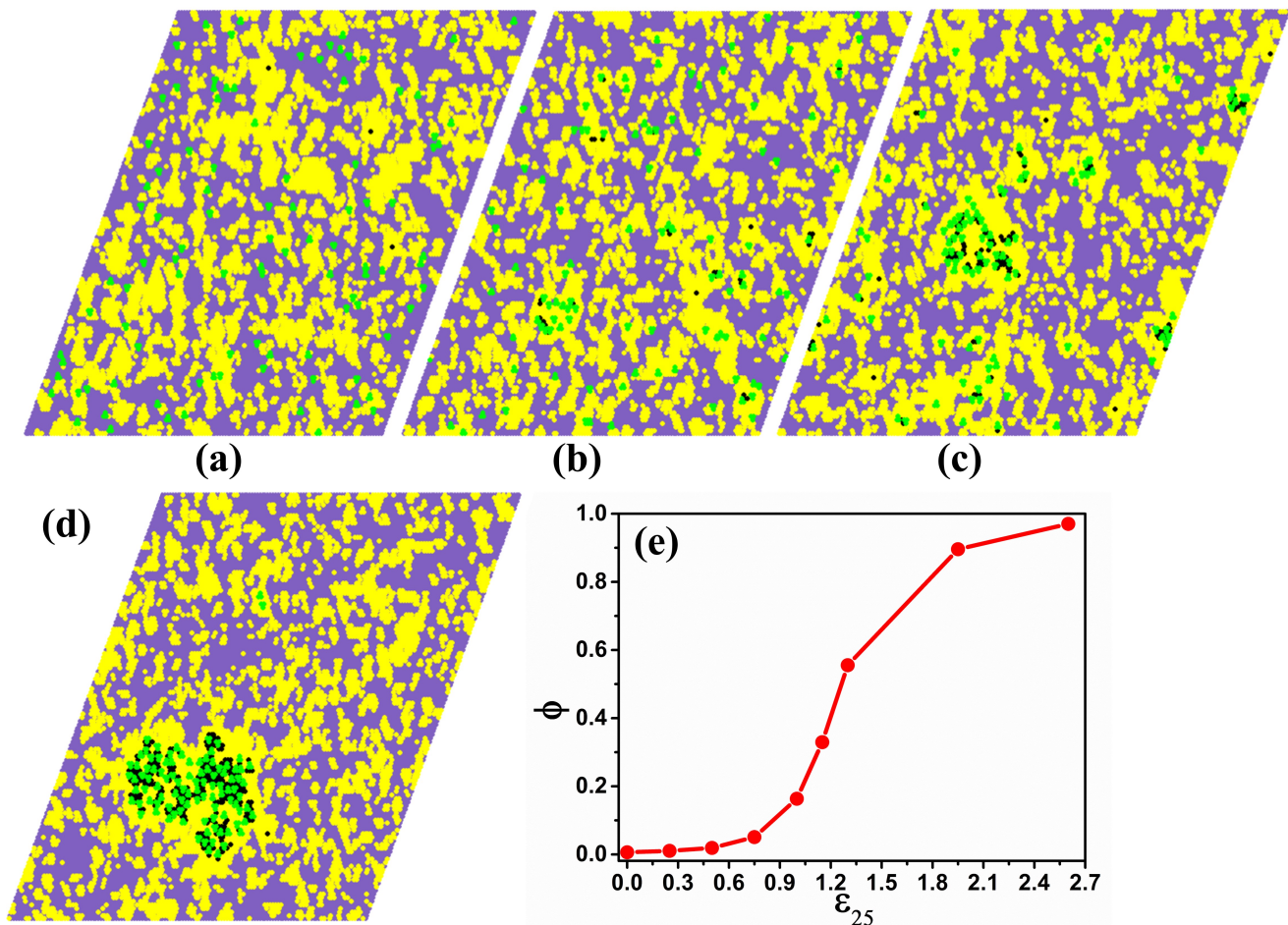


FIG. 3. Partitioning of proteins in DPPC/DOPC/Chol mixture in one-phase region (12DPPC) for varying strength of  $\epsilon_{25}$ . Snapshots (a)-(d) show equilibrium distributions of systems corresponding to  $\epsilon_{25} = 0, 1.0\epsilon, 1.3\epsilon,$  and  $1.95\epsilon$ , respectively. Color coding the same as in fig. 2. (e) The fraction,  $0 \leq \phi \leq 1$  of the proteins completely inside the  $L_o$  phase, as a function of  $\epsilon_{25}$ . The line is a guide to the eye.

amount of proteins can change this local organization dramatically and, as shown below, may lead to the formation of much larger domains. This is interesting in light of the question lingering about the formation and sizes of liquid-ordered domains in model mixtures at physiological temperature 37C, and the role played by the proteins in the assembly and growth of raft domains in biological membranes.<sup>99,100</sup>

Computational results from the simulations of the one-phase 12DPPC mixture are displayed in fig. 3. The trend in the partitioning behavior of proteins is quite similar to the behavior in fig. 2 of the macroscopically phase-separated 35DPPC mixture. The fraction of proteins in the liquid-ordered domains increases with the interaction free energy,  $\epsilon_{25}$ , between them and ordered DPPC chains. This is evident from the sequence of equilibrium snapshots fig. 3(a)-(d), corresponding to  $\epsilon_{25} = 0, 1.0\epsilon, 1.3\epsilon,$  and  $1.95\epsilon$ , respectively, as well as from fig. 3(e) showing the fraction of proteins fully residing in the liquid-ordered domains. Notice that, in comparison to the two-phase region (fig. 2), the transition of the proteins from the disordered to the ordered regions in the one-phase system occurs at higher values of  $\epsilon_{25}$ , which is antic-

ipated since the fraction of saturated DPPC lipids is smaller. Also, because the system separates locally rather than macroscopically, there is a larger interfacial contact line between the liquid phases and, therefore, a higher fraction of proteins reside between them rather than inside the liquid-ordered regions.

An interesting observation is that, together with the gradual migration of the proteins into the liquid-ordered domains at higher values of  $\epsilon_{25}$ , larger domains surrounding the proteins begin to appear in the mixture. This trend can be observed in the snapshot in fig. 3(c) corresponding to  $\epsilon_{25} = 1.3\epsilon$ , showing several larger protein-containing domains. By following the dynamics of the system (see Supplementary Material, SI movie 12DPPC\_1.3.mp4), it can be concluded that these are metastable dynamic domains: Their shapes and sizes constantly change as they form, sometimes merge with other domains, and eventually disintegrate.

Larger and more stable domains are obtained for higher values of  $\epsilon_{25} = 1.95\epsilon$ , see fig. 3(d). The sequence of snapshots in fig. 4 show how a single large domain that contains almost all the proteins dispersed in the system, evolves via the coa-

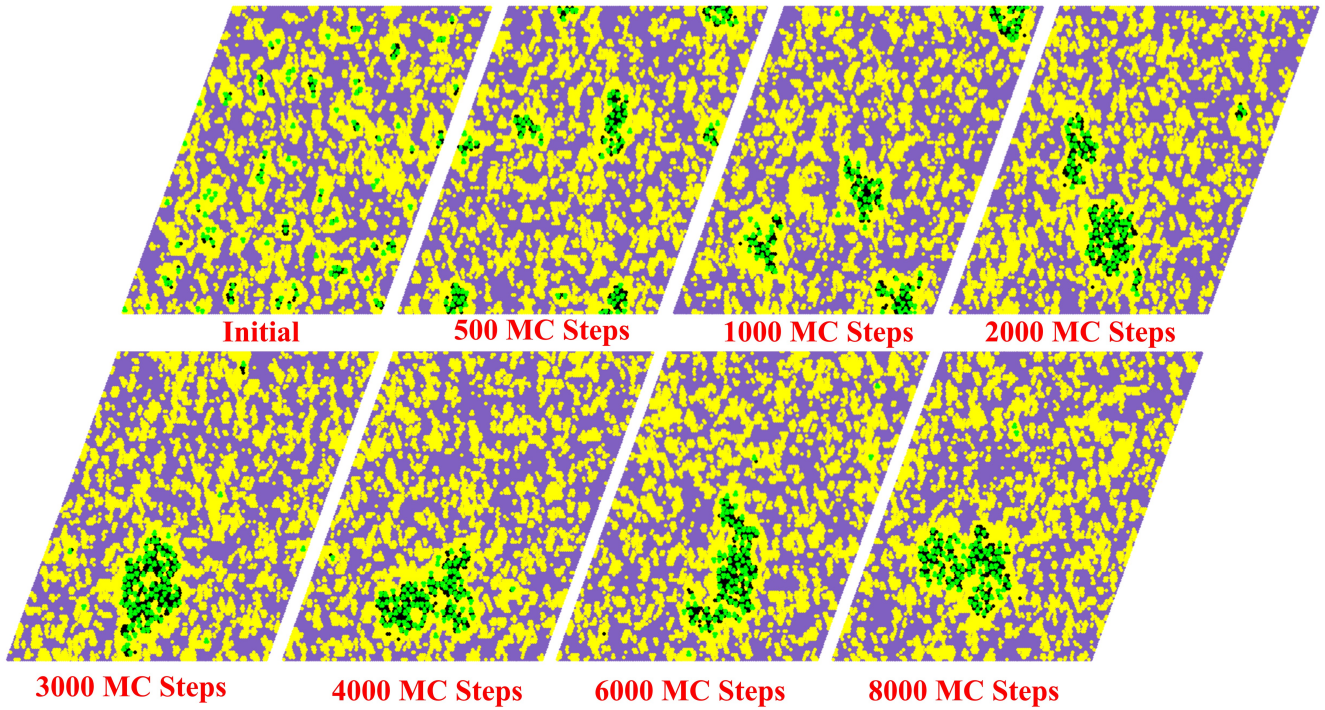


FIG. 4. A sequence showing the temporal evolution and the formation of a large cluster containing almost all the proteins in a 12DPPC mixture with  $\epsilon_{25} = 1.95\epsilon$ . Color coding as in fig. 2.

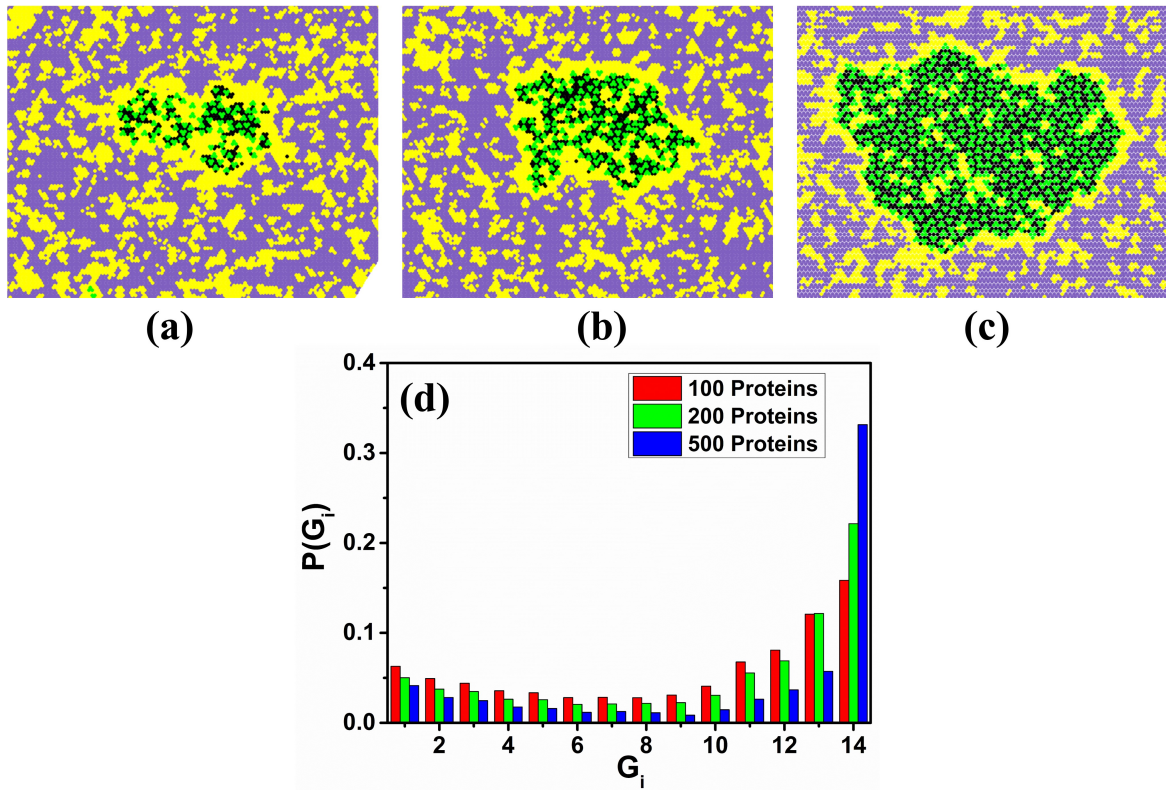


FIG. 5. Equilibrium snapshots showing the large ordered domain formed in 12DPPC mixtures with  $\epsilon_{25} = 1.95\epsilon$  and (a) 100, (b) 200, and (c) 500 proteins. (d) The distribution histogram of the values of order parameter  $G_i$  of the sites belonging to the large ordered domain.

lescence of smaller domains (see Supplementary Material, SI movie 12DPPC\_1.95.mp4). This observation marks the fundamental difference between the two-phase 35DPPC mixture discussed above, and the one-phase 12DPPC mixture. In both cases the proteins show affinity to the DPPC-rich ordered domains, but in the latter case they also change the lipid distribution in the mixture. The formation of a single large domain suggests that the addition of a small density of proteins with strong affinity to the saturated lipids can induce phase separation between a  $L_o$  phase that is rich in proteins and saturated lipids, and a  $L_d$  phase with nanometric ordered domains, which is DPPC-poor and completely depleted of proteins. The fact that, despite a clear loss of mixing entropy, the proteins are not dispersed in the many liquid-ordered nanometric domains but aggregate in a single larger domain, is a clear indication that the mixture undergoes a phase transition that is driven by the attractive interaction between the proteins and the ordered saturated chains.

The size of the large domain is limited by the amount of the available proteins, as can be seen in the snapshots in fig. 5, showing equilibrium configurations of 12DPPC mixtures with  $\epsilon_{25} = 1.95\epsilon$  and with (a) 100, (b) 200, and (c) 500 proteins, respectively. The growth in the size of the large domain is not only due to the addition of proteins to the mixture, but also because of the recruitment of DPPC lipids. About 40% of them are found in the large ordered domain in (a), and this fraction grows to  $\approx 60\%$  and  $\approx 90\%$  in (b) and (c), respectively. In contrast, the partition of the other components between the large domain and the surrounding does not change with the addition of proteins, and we find that less than 3% of the DOPC lipids and  $\approx 13\%$  of the Chol molecules are in the ordered domain. Thus, the composition *within* the large domain is different in snapshots fig. 5 (a)-(c), implying that the phase of the domain may be also different. One of the hallmarks of the  $L_o$  phase is the existence of gel-like nano-clusters<sup>58,59</sup>, which in the absence of proteins (i.e., for mixtures containing only lipids) are composed of tightly packed saturated lipids. In mixtures also containing proteins with strong affinity to saturated lipids, these nano-clusters are nucleated around the proteins, as can be seen in fig. 5 (a) by the overlap between the locations of the proteins (marked by green color) and the gel-like regions (marked by black). With the addition of more proteins to the system and the corresponding changes in the composition of the large domain, the phase changes gradually from  $L_o$  (liquid-ordered) in fig. 5 (a) to  $S_o$  (gel) in fig. 5 (c). This trend is summarized in fig. 5 (d), showing the distribution histograms of the values of the order parameter  $G_i$  [Eq. (2)] in the large ordered domain. In all three cases corresponding to different numbers of proteins, a significant fraction of the domain sites are associated with the gel state ( $G_i = 14$ ). This number grows markedly with the number of proteins, which indicates the transformation of the ordered domain from a liquid-ordered to gel phase.

To summarize, proteins with sufficiently strong attraction to saturated lipids (stronger than the attraction of the lipids to each other) can drive the system to phase separate by serving as nucleation centers for the formation of liquid-ordered domains. This mechanism has been speculated by experimental

works,<sup>101,102</sup> and has been demonstrated in previous ultra CG and lattice simulations.<sup>94</sup> At lower affinities and low densities of proteins, the system may still exhibit metastable dynamic domains whose size may be comparable to lipid rafts in complex biological membranes.

Fig. 6 shows equilibrium configurations of the 18DPPC mixture, where the largest ordered cluster is colored by red. The snapshots in (a)-(e) correspond to  $\epsilon_{25} = 0, 0.75\epsilon, 1.3\epsilon, 1.95\epsilon$ , and  $2.6\epsilon$ , respectively. The main difference between the 18DPPC mixture and the 12DPPC mixture is that the former is located close to the phase boundary separating the one- and two-phase regions (see fig. 1). Therefore, the ordered domains appearing in snapshots (a) and (b) are larger than those appearing for similar values of  $\epsilon_{25}$  at 12DPPC. They look branched and resemble percolation clusters that tend to form when mixtures are in the vicinity of the phase transition critical point. Other than this, the system behaves quite similarly to the 12DPPC mixture: It undergoes phase separation when the attraction of the proteins to the DPPC lipids is stronger than the affinity of the lipids to each other. The phase transition can be read from the distribution histograms of the values of the order parameter  $G_i$  shown in fig. 7. These histograms are computed for the entire mixture (not only for the largest ordered domain, as in fig. 5) for 18DPPC mixture with no proteins, and with 100 proteins with  $\epsilon_{25} = 0.75\epsilon$ , and  $\epsilon_{25} = 1.95\epsilon$ . In the first two histograms, only a tiny fraction of the system is identified as gel-like. In the third case (100 proteins with  $\epsilon_{25} = 1.95\epsilon$ ), the bimodal nature of the distribution is evident, with the second peak at high values of  $G_i$  (including a growing fraction of gel-like sites with the maximum value  $G_i = 14$ ). As noted above, this is a characteristic feature of the  $L_o$  phase. More information about the structural changes associated with the transition to two-phase separation can be found in table II, where details about the composition and structure of the largest ordered domain are provided. The data highlights two major differences between the large domains in the one-phase ( $\epsilon_{25} = 0$  and  $0.75\epsilon$ ) and the two-phase cases ( $\epsilon_{25} = 1.3\epsilon$  and  $1.95\epsilon$ ). One is the fact that in the two-phase case, the proteins are found in the  $L_o$  large domain, whereas in the one-phase region, they are distributed in the entire mixture. The  $L_o$  domain in the two-phase region also attracts a larger fraction of the saturated DPPC lipids. These trends were also observed in the 12DPPC mixture discussed above. The other notable observation from the table is related to the size (gyration radius) of the largest domain. The striking piece of information is not the steady growth in the size of the domain with  $\epsilon_{25}$  [ $R_g$  (mean)], but the standard deviation [ $R_g$  (SD)] which measures the characteristic fluctuations in the domain size. The data reflects the stability of the  $L_o$  phase domain in the two-phase region where the size of the ordered domain is nearly constant vs. the dynamic nature of the ‘‘percolation’’ domain in the one-phase region whose size varies considerably in time.



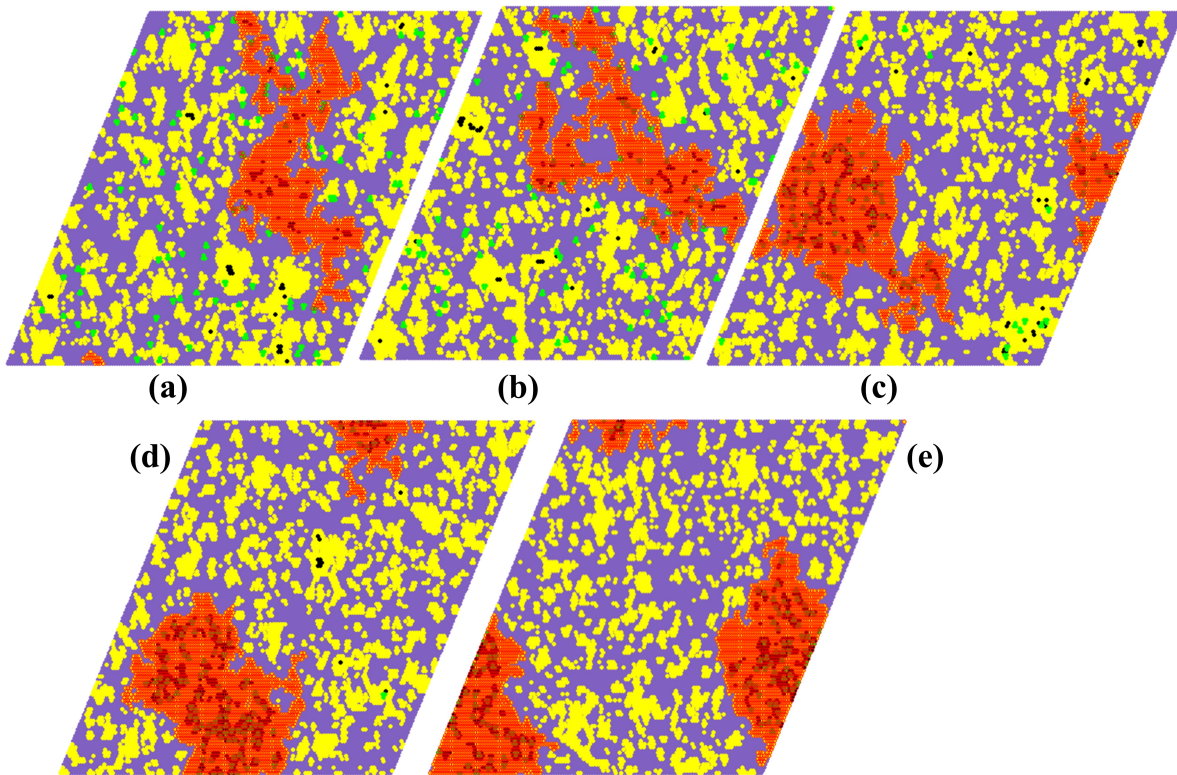


FIG. 6. Equilibrium configurations of 18DPPC mixture with  $\epsilon_{25} = 0$  (a),  $0.75\epsilon$  (b),  $1.3\epsilon$  (c),  $1.95\epsilon$  (d), and  $2.6\epsilon$  (e). The mixture contains 100 proteins. Color coding as in fig. 2, except for the largest ordered domain in the mixture, which is colored by red.

TABLE II. Fractions of proteins and DPPC lipids partitioned in the large ordered domain, and data on its gyration radius,  $R_g$ , in 18DPPC mixtures, as a function of  $\epsilon_{25}$ .

$\epsilon_{25}$	% Protein	% DPPC	$R_g$ (Mean) (Å)	$R_g$ (SD) (Å)
0.0	$5.0 \pm 2.5$	$23.0 \pm 7.0$	167	67
0.75	$14.5 \pm 6.0$	$19.0 \pm 7.0$	229	93
1.30	$87.0 \pm 6.0$	$40.0 \pm 4.5$	263	15
1.95	$98.5 \pm 1.0$	$52.0 \pm 2.5$	358	8

#### IV. CONCLUSIONS

Ternary mixtures of saturated and unsaturated lipids with Chol serve as minimal model systems for studying phase separation in complex biological membranes. Under suitable conditions, they exhibit coexistence of liquid-ordered domains with a liquid-disordered matrix. This phase behavior is believed to be relevant to lipid rafts, which are dynamic liquid-ordered domains of typical size of several tens of nanometers, that “float” on the cell surface.

Lipid rafts contain certain proteins that are involved in different biological processes. Here, we extended a previously published lattice model of ternary DPPC/DOPC/Chol mixtures to include small proteins (peptides). We perform extensive MC simulations to investigate two closely-related phenomena - the impact of the proteins on the phase behavior, and the distribution of the proteins between the liquid phases. We focus on, so called, Type II mixtures, i.e., mixtures that in the

absence of proteins exhibit macroscopic liquid-liquid phase separation. The proteins in our simulations do not interact directly with each other. Thus, the extension of the model involves the addition of only a single interaction parameter,  $\epsilon_{25}$ , corresponding to the affinity between the proteins and the saturated ordered lipid chains. In future works we plan to extend our investigations of Type I mixtures, which in our previous studies<sup>59,95</sup> were observed when the model parameter  $\epsilon_{24}$  was set to a value larger than  $0.3\epsilon$ . Fig. 8 shows preliminary results from ongoing Type I mixture simulations for  $\epsilon_{24} = 0.4\epsilon$ . Fig. 8(a) is a 12DPPC type I mixture at  $\epsilon_{25} = 1.95\epsilon$ , and is remarkably similar to fig. 3(d) which shows the type II mixture with the same model parameters except for the value of  $\epsilon_{24}$ . In contrast, fig. 8(b) displays a type I 35DPPC mixture, which looks markedly different than its type II counterpart shown in fig. 2(c). This difference may not be surprising considering that the main difference between Type I and Type II mixtures is in the two-phase region.

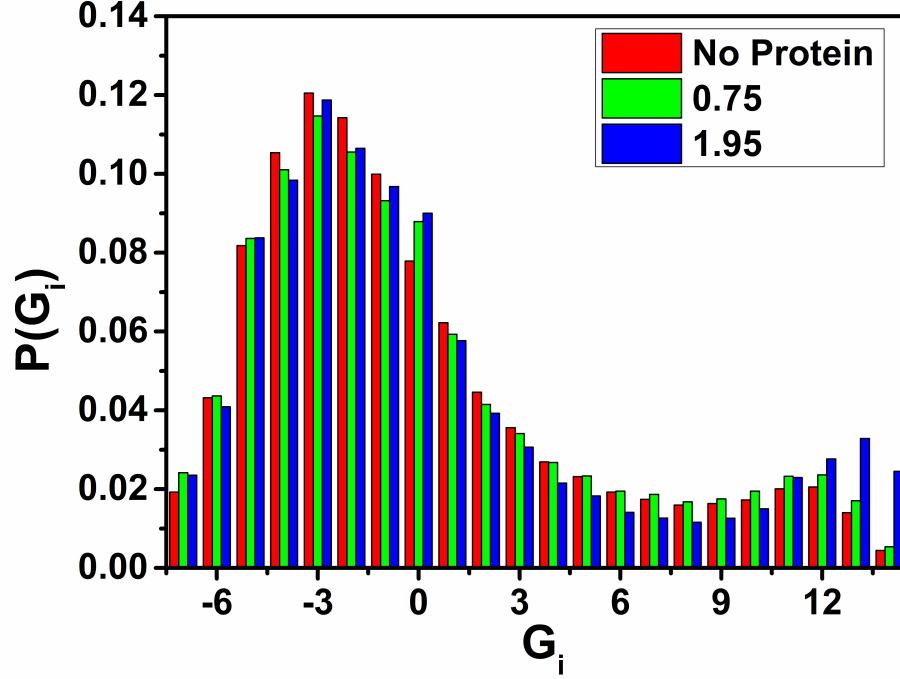


FIG. 7. The distribution histogram of the values of order parameter  $G_i$  of 18DPPC mixtures with no proteins, 100 proteins with  $\epsilon_{25} = 0.75\epsilon$ , 100 proteins with  $\epsilon_{25} = 1.95\epsilon$ .

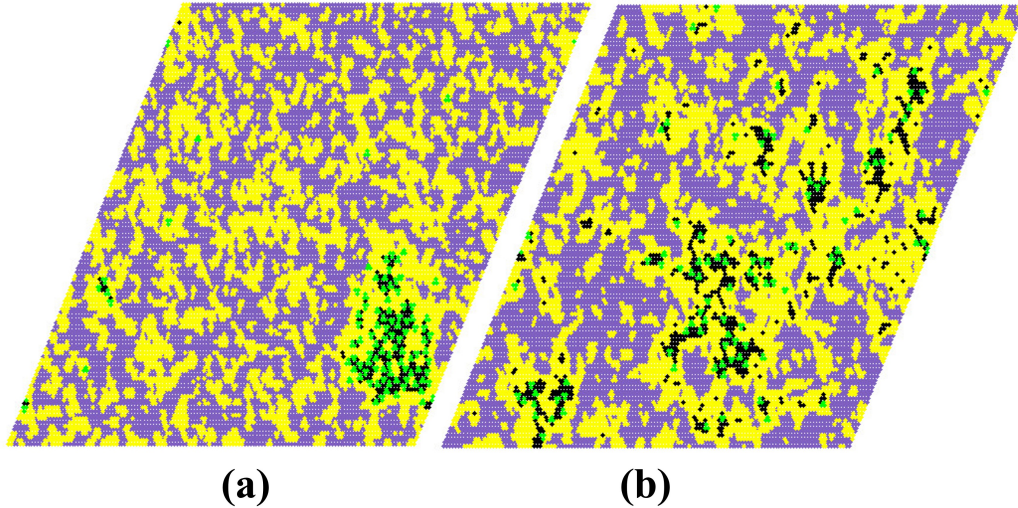


FIG. 8. Equilibrium snapshots of Type I mixtures with  $\epsilon_{24} = 0.4\epsilon$ . (a) and (b) show 12DPPC and 35DPPC mixtures, respectively, In both cases, we set  $\epsilon_{25} = 1.95\epsilon$ .

In addition to changing the Type of the mixture by variations of the model parameter  $\epsilon_{24}$ , we also consider performing simulations with other model parameters like  $\epsilon_{35}$  (Chol-peptide) and  $\epsilon_{45}$  (DOPC-peptide), which should lead to an even richer phase behavior. A particularly interesting example is of mixtures where the peptides have no strong affinity

to either of the liquid phases, but rather favor the proximity of the Chol which tend to be present in both of them.

Not surprisingly, we find that the migration of proteins into the liquid-ordered domains depends strongly on  $\epsilon_{25}$ . More precisely, since proteins embedded in liquid-ordered domains take the place of saturated lipids and Chol, their partition into

the DPPC-rich  $L_o$  phase depends on the associate exchange parameter. This is the reason why the partition behavior of the proteins changes rapidly when  $\epsilon_{25} \simeq \epsilon_{22} = 1.3\epsilon$ , as can be seen in fig. 2 summarizing our results from simulations of mixtures in the two-phase region. Model proteins with low affinity to saturated lipids remain in the DPPC-poor  $L_d$  phase and, conversely, when  $\epsilon_{25} > \epsilon_{22}$  they accumulate in the DPPC-rich  $L_o$  phase.

At low compositions of saturated DPPC lipids, the ternary mixture is one phase which is predominantly liquid-disordered, with local density fluctuations appearing as liquid-ordered domains of nanometric scale. These dynamic domains are 1-1.5 order of magnitude smaller than lipid rafts. The presence of proteins in biological membranes has been mentioned as one of the factors contributing to the growth and meta-stability of lipid rafts. Our model simulations reveal that the presence of even a small density of small non-interacting peptides can, indeed, lead to dramatic changes in these properties of the liquid-ordered domains formed in ternary mixtures. We find (see fig. 3) that with the increase in the affinity parameter  $\epsilon_{25}$ , the liquid ordered domains grow in size by recruiting proteins and saturated lipids. These large liquid-ordered domains become increasingly metastable and begin to develop gel-like clusters which are blends of lipids and ordered saturated lipid chains. Eventually, when the affinity between the proteins and saturated lipids exceeds the affinity of the saturated lipids to each other, the liquid-ordered domains merge into a single distinct stable phase containing most of the proteins. Depending on the relative proportions of proteins and saturated lipids, the phase separated from the  $L_d$  environment may be either  $L_o$  or  $S_o$  (see fig. 5). The biologically most relevant result may be the behavior of the 18DPPC mixtures when  $\epsilon_{25} \lesssim \epsilon_{22}$  [see, e.g., fig. 6, snapshots (b)-(c)]. There, near the critical point of the ternary mixture, the presence of low density of proteins, can lead to the formation of metastable dynamic liquid-ordered domains whose size is comparable to the size of lipid rafts (see Supplementary Material, SI movie 18DPPC\_1.3.mp4).

We conclude by reminding the reader that cell membranes are larger and far more complex than the model mixtures studied herein. They include larger proteins of different kinds, and their dynamic behavior depends on many more factor, including non-equilibrium contributions arising, e.g., from their interactions with the cell cytoskeleton. Different regions of these membrane may be effectively subject to different local compositions and interactions. Our study shows that even a simple mixture model with a small number of interaction parameters, may exhibit rich equilibrium phase behavior with characteristics resembling key features of lipid rafts.

## SUPPLEMENTARY MATERIAL

See supplementary material for movies showing the dynamics of different mixtures.

## ACKNOWLEDGMENTS

This work was supported by the Israel Science Foundation (ISF), grant No. 1258/22.

## DATA AVAILABILITY STATEMENT

The data validating the findings of our simulation study are available upon request to the corresponding author.

## CONFLICT OF INTEREST

The authors declare no conflict of interest.

## AUTHOR CONTRIBUTIONS

**SB:** Software; Data curation; Analysis; Writing. **OF:** Conceptualization; supervision; Funding Acquisition; Writing.

- <sup>1</sup>B. Alberts, *Molecular biology of the cell* (WW Norton & Company, 2017).
- <sup>2</sup>X. Cheng and J. C. Smith, *Chem. Rev.* **119**, 5849 (2019).
- <sup>3</sup>A. Shevchenko and K. Simons, *Nat. Rev. Mol. Cell Biol.* **11**, 593 (2010).
- <sup>4</sup>Y. xiao Shen, P. O. Saboe, I. T. Sines, M. Erbakan, and M. Kumar, *J. Membr. Sci.* **454**, 359 (2014).
- <sup>5</sup>A. Blanco and G. Blanco, in *Med. Biochem.*, edited by A. Blanco and G. Blanco (Academic Press, 2017) pp. 215–250.
- <sup>6</sup>G. Guigas and M. Weiss, *Biochim. Biophys. Acta, Biomembr.* **1858**, 2441 (2016).
- <sup>7</sup>W. N. Konings, H. R. Kaback, and J. S. Lolkema, *Transport processes in eukaryotic and prokaryotic organisms* (Elsevier, 1996).
- <sup>8</sup>M. Jelokhani-Niaraki, “Membrane proteins: structure, function and motion,” (2022).
- <sup>9</sup>D. Whitford, *Proteins: structure and function* (John Wiley & Sons, 2013).
- <sup>10</sup>S. Sj, *Science* **175**, 720 (1972).
- <sup>11</sup>S. N. Ahmed, D. A. Brown, and E. London, *Biochemistry* **36**, 10944 (1997).
- <sup>12</sup>D. A. Brown and J. K. Rose, *Cell* **68**, 533 (1992).
- <sup>13</sup>A. Pralle, P. Keller, E.-L. Florin, K. Simons, and J. H. Hörber, *J. Cell Biol.* **148**, 997 (2000).
- <sup>14</sup>D. G. Ackerman and G. W. Feigenson, *Essays Biochem.* **57**, 33 (2015).
- <sup>15</sup>J. Huang and G. W. Feigenson, *Biophys. J.* **76**, 2142 (1999).
- <sup>16</sup>S. Schuck, M. Honsho, K. Ekroos, A. Shevchenko, and K. Simons, *Proc. Natl. Acad. Sci.* **100**, 5795 (2003).
- <sup>17</sup>L. J. Pike, *J. Lipid Res.* **47**, 1597 (2006).
- <sup>18</sup>O. G. Mouritsen, *Biochim. Biophys. Acta, Biomembr.* **1798**, 1286 (2010).
- <sup>19</sup>A. Filippov, G. Orädd, and G. Lindblom, *Biophys. J.* **86**, 891 (2004).
- <sup>20</sup>M. M. B. Holl, “Cell plasma membranes and phase transitions,” in *Phase Transitions in Cell Biology*, edited by G. H. Pollack and W.-C. Chin (Springer Netherlands, Dordrecht, 2008) pp. 171–181.
- <sup>21</sup>D. Marsh, *Handbook of lipid bilayers* (CRC press, 2013).
- <sup>22</sup>G. W. Feigenson, *Biochim. Biophys. Acta, Biomembr.* **1788**, 47 (2009).
- <sup>23</sup>S. Komura and D. Andelman, *Adv. Colloid Interface Sci.* **208**, 34 (2014).
- <sup>24</sup>S. L. Veatch, O. Soubias, S. L. Keller, and K. Gawrisch, *Proc. Natl. Acad. Sci.* **104**, 17650 (2007).
- <sup>25</sup>L. S. Hirst, P. Uppamoochikkal, and C. Lor, *Liq. Cryst.* **38**, 1735 (2011).
- <sup>26</sup>M. Stöckl and A. Herrmann, *Biochim. Biophys. Acta, Biomembr.* **1798**, 1444 (2010).
- <sup>27</sup>L. A. Bagatolli and E. Gratton, *J. Fluoresc.* **11**, 141 (2001).
- <sup>28</sup>L. A. Bagatolli and E. Gratton, *Biophys. J.* **79**, 434 (2000).
- <sup>29</sup>O. Farago, in *Modeling Biomaterials* (Springer, 2021) pp. 1–41.
- <sup>30</sup>A. Koukalová, M. Amaro, G. Aydogan, G. Gröbner, P. T. Williamson, I. Mikhalyov, M. Hof, and R. Šachl, *Sci. Rep.* **7**, 5460 (2017).

- <sup>31</sup>R. F. de Almeida, L. M. Loura, A. Fedorov, and M. Prieto, *J. Mol. Biol.* **346**, 1109 (2005).
- <sup>32</sup>R. Šachl, J. Humpolíčková, M. Štefl, L. B.-Å. Johansson, and M. Hof, *Biophys. J.* **101**, L60 (2011).
- <sup>33</sup>G. De Wit, J. S. Daniai, P. Kukura, and M. I. Wallace, *Proc. Natl. Acad. Sci.* **112**, 12299 (2015).
- <sup>34</sup>M.-C. Giocondi, V. Vié, E. Lesniewska, P.-E. Milhiet, M. Zinke-Allmang, and C. Le Grimellec, *Langmuir* **17**, 1653 (2001).
- <sup>35</sup>F. Tokumasu, A. J. Jin, G. W. Feigenson, and J. A. Dvorak, *Biophys. J.* **84**, 2609 (2003).
- <sup>36</sup>A. Choucair, M. Chakrapani, B. Chakravarthy, J. Katsaras, and L. Johnston, *Biochim. Biophys. Acta, Biomembr.* **1768**, 146 (2007).
- <sup>37</sup>S. L. Veatch, I. Polozov, K. Gawrisch, and S. L. Keller, *Biophys. J.* **86**, 2910 (2004).
- <sup>38</sup>S. J. Marrink, V. Corradi, P. C. Souza, H. I. Ingólfsson, D. P. Tieleman, and M. S. Sansom, *Chem. Rev.* **119**, 6184 (2019).
- <sup>39</sup>W. D. Bennett and D. P. Tieleman, *Biochim. Biophys. Acta, Biomembr.* **1828**, 1765 (2013).
- <sup>40</sup>W. D. Bennett and D. P. Tieleman, *Biochim. Biophys. Acta, Biomembr.* **1828**, 1765 (2013).
- <sup>41</sup>M. Javanainen, H. Martinez-Seara, and I. Vattulainen, *Sci. Rep.* **7**, 1143 (2017).
- <sup>42</sup>A. J. Sodt, M. L. Sandar, K. Gawrisch, R. W. Pastor, and E. Lyman, *J. Am. Chem. Soc.* **136**, 725 (2014).
- <sup>43</sup>A. J. Sodt, R. W. Pastor, and E. Lyman, *Biophys. J.* **109**, 948 (2015).
- <sup>44</sup>Z. Cournia, G. M. Ullmann, and J. C. Smith, *J. Phys. Chem. B* **111**, 1786 (2007).
- <sup>45</sup>D. Hakobyan and A. Heuer, *J. Phys. Chem. B* **117**, 3841 (2013).
- <sup>46</sup>W. D. Bennett, J.-E. Shea, and D. P. Tieleman, *Biophys. J.* **114**, 2595 (2018).
- <sup>47</sup>R.-X. Gu, S. Baoukina, and D. P. Tieleman, *J. Am. Chem. Soc.* **142**, 2844 (2020).
- <sup>48</sup>J. D. Perlmutter and J. N. Sachs, *J. Am. Chem. Soc.* **131**, 16362 (2009).
- <sup>49</sup>C. Rosetti and C. Pastorino, *J. Phys. Chem. B* **116**, 3525 (2012).
- <sup>50</sup>R. S. Davis, P. Sunil Kumar, M. M. Sperotto, and M. Laradji, *J. Phys. Chem. B* **117**, 4072 (2013).
- <sup>51</sup>S. Baoukina, E. Mendez-Villuendas, W. D. Bennett, and D. P. Tieleman, *Faraday Discuss.* **161**, 63 (2013).
- <sup>52</sup>G. A. Pantelopulos and J. E. Straub, *Biophys. J.* **115**, 2167 (2018).
- <sup>53</sup>C. Arnarez, A. Webb, E. Rouvière, and E. Lyman, *J. Phys. Chem. B* **120**, 13086 (2016).
- <sup>54</sup>Y. Wang, P. Gkeka, J. E. Fuchs, K. R. Liedl, and Z. Cournia, *Biochim. Biophys. Acta, Biomembr.* **1858**, 2846 (2016).
- <sup>55</sup>S. He and L. Maibaum, *J. Phys. Chem. B* **122**, 3961 (2018).
- <sup>56</sup>T. S. Carpenter, C. A. López, C. Neale, C. Montour, H. I. Ingólfsson, F. Di Natale, F. C. Lightstone, and S. Gnanakaran, *J. Chem. Theory Comput* **14**, 6050 (2018).
- <sup>57</sup>M. Podewitz, Y. Wang, P. Gkeka, S. von Grafenstein, K. R. Liedl, and Z. Cournia, *J. Phys. Chem. B* **122**, 10505 (2018).
- <sup>58</sup>T. Sarkar and O. Farago, *Phys. Rev. Res.* **3**, L042030 (2021).
- <sup>59</sup>T. Sarkar and O. Farago, *Soft Matter* **19**, 2417 (2023).
- <sup>60</sup>S. Meinhardt and F. Schmid, *Soft Matter* **15**, 1942 (2019).
- <sup>61</sup>P. F. Almeida, *Biophys. J.* **100**, 420 (2011).
- <sup>62</sup>D. Lingwood and K. Simons, *science* **327**, 46 (2010).
- <sup>63</sup>M. B. Stone, S. A. Shelby, M. F. Núñez, K. Wisser, and S. L. Veatch, *elife* **6**, e19891 (2017).
- <sup>64</sup>D. I. Danylchuk, E. Sezgin, P. Chabert, and A. S. Klymchenko, *Anal. Chem.* **92**, 14798 (2020).
- <sup>65</sup>K. Beck-García, E. Beck-García, S. Bohler, C. Zorzin, E. Sezgin, I. Levental, B. Alarcón, and W. W. Schamel, *Biochim. Biophys. Acta, Mol. Cell Res.* **1853**, 802 (2015).
- <sup>66</sup>F. Magnani, C. G. Tate, S. Wynne, C. Williams, and J. Haase, *J. Biol. Chem.* **279**, 38770 (2004).
- <sup>67</sup>L. K. Cuddy, W. Winick-Ng, and R. J. Rylett, *J. Neurochem.* **128**, 725 (2014).
- <sup>68</sup>C.-s. Huang, J. Zhou, A. K. Feng, C. C. Lynch, J. Klumperman, S. J. DeArmond, and W. C. Mobley, *J. Biol. Chem.* **274**, 36707 (1999).
- <sup>69</sup>J. Bodoso, S. S. Iyer, and A. Srivastava, *J. Membr. Biol.* **253**, 551 (2020).
- <sup>70</sup>S. Kedia, P. Ramakrishna, P. R. Netrakanti, M. Jose, J.-B. Sibarita, S. Nadkarni, and D. Nair, *Nanoscale* **12**, 8200 (2020).
- <sup>71</sup>J. Colin, L. Gregory-Pauron, M.-C. Lanhers, T. Claudepierre, C. Corbier, F. T. Yen, C. Malaplate-Armand, and T. Oster, *Biochim.* **130**, 178 (2016).
- <sup>72</sup>P. Sengupta, A. Y. Seo, H. A. Pasolli, Y. E. Song, M. C. Johnson, and J. Lippincott-Schwartz, *Nat. Cell Biol* **21**, 452 (2019).
- <sup>73</sup>S.-T. Yang, A. J. Kreutzberger, V. Kiessling, B. K. Ganser-Pornillos, J. M. White, and L. K. Tamm, *Sci. Adv.* **3**, e1700338 (2017).
- <sup>74</sup>S.-T. Yang, V. Kiessling, and L. K. Tamm, *Nat. Commun.* **7**, 11401 (2016).
- <sup>75</sup>L. V. Schäfer, D. H. de Jong, A. Holt, A. J. Rzepiela, A. H. de Vries, B. Poolman, J. A. Killian, and S. J. Marrink, *Proc. Natl. Acad. Sci.* **108**, 1343 (2011).
- <sup>76</sup>H.-J. Kaiser, A. Orłowski, T. Róg, T. K. Nyholm, W. Chai, T. Feizi, D. Lingwood, I. Vattulainen, and K. Simons, *Proc. Natl. Acad. Sci.* **108**, 16628 (2011).
- <sup>77</sup>X. Periole, T. Huber, S.-J. Marrink, and T. P. Sakmar, *J. Am. Chem. Soc.* **129**, 10126 (2007).
- <sup>78</sup>J. Domański, S. J. Marrink, and L. V. Schäfer, *Biochim. Biophys. Acta, Biomembr.* **1818**, 984 (2012), protein Folding in Membranes.
- <sup>79</sup>D. H. de Jong, C. A. Lopez, and S. J. Marrink, *Faraday Discuss.* **161**, 347 (2013).
- <sup>80</sup>L. Janosi, Z. Li, J. F. Hancock, and A. A. Gorfe, *Proc. Natl. Acad. Sci.* **109**, 8097 (2012).
- <sup>81</sup>J. Lorent, K. R. Levental, L. Ganesan, G. Rivera-Longsworth, E. Sezgin, M. Doktorova, E. Lyman, and I. Levental, *Nat. Chem. Biol* **16**, 644 (2020).
- <sup>82</sup>X. Lin, A. A. Gorfe, and I. Levental, *Biophys. J.* **114**, 1936 (2018).
- <sup>83</sup>J. Bodoso, S. S. Iyer, and A. Srivastava, *J. Membr. Biol.* **253**, 551 (2020).
- <sup>84</sup>J. H. Lorent, B. Diaz-Rohrer, X. Lin, K. Spring, A. A. Gorfe, K. R. Levental, and I. Levental, *Nat. Commun.* **8**, 1219 (2017).
- <sup>85</sup>I. Levental, M. Grzybek, and K. Simons, *Biochemistry* **49**, 6305 (2010).
- <sup>86</sup>C. L. Nilsson, in *Lectins*, edited by C. L. Nilsson (Elsevier Science B.V., Amsterdam, 2007) pp. 1–13.
- <sup>87</sup>M. Cebecauer, M. Amaro, P. Jurkiewicz, M. J. Sarmiento, R. Sachl, L. Cwiklik, and M. Hof, *Chem. Rev.* **118**, 11259 (2018).
- <sup>88</sup>D. Marsh, *Biochim. Biophys. Acta, Biomembr.* **1778**, 1545 (2008).
- <sup>89</sup>P. S. Niemela, M. S. Miettinen, L. Monticelli, H. Hammaren, P. Bjelkmar, T. Murtola, E. Lindahl, and I. Vattulainen, *J. Am. Chem. Soc.* **132**, 7574 (2010).
- <sup>90</sup>O. G. Mouritsen and M. Bloom, *Biophys. J.* **46**, 141 (1984).
- <sup>91</sup>A. Kusumi, C. Nakada, K. Ritchie, K. Murase, K. Suzuki, H. Murakoshi, R. S. Kasai, J. Kondo, and T. Fujiwara, *Annu. Rev. Biophys. Biomol. Struct.* **34**, 351 (2005).
- <sup>92</sup>M. M. Sperotto, J. H. Ipsen, and O. G. Mouritsen, *Cell Biophys* **14**, 79 (1989).
- <sup>93</sup>A. Hinderliter, P. F. Almeida, C. E. Creutz, and R. L. Biltonen, *Biochemistry* **40**, 4181 (2001).
- <sup>94</sup>M. Hoferer, S. Bonfanti, A. Taloni, C. A. La Porta, and S. Zapperi, *Phys. Rev. E* **100**, 042410 (2019).
- <sup>95</sup>T. Sarkar and O. Farago, *Eur. Phys. J. E* **46**, 99 (2023).
- <sup>96</sup>S. L. Veatch and S. L. Keller, *Phys. Rev. Lett.* **94**, 148101 (2005).
- <sup>97</sup>S. L. Veatch and S. L. Keller, *Biophys. J.* **85**, 3074 (2003).
- <sup>98</sup>J. Hoshen and R. Kopelman, *Phys. Rev. B* **14**, 3438 (1976).
- <sup>99</sup>A. Kusumi, T. K. Fujiwara, T. A. Tsunoyama, R. S. Kasai, A.-A. Liu, K. M. Hirotsawa, M. Kinoshita, N. Matsumori, N. Komura, H. Ando, *et al.*, *Traffic* **21**, 106 (2020).
- <sup>100</sup>C. M. Rosetti, A. Mangiarotti, and N. Wilke, *Biochim. Biophys. Acta, Biomembr.* **1859**, 789 (2017).
- <sup>101</sup>E. Sezgin, I. Levental, S. Mayor, and C. Eggeling, *Nat. Rev. Mol. Cell Biol.* **18**, 361 (2017).
- <sup>102</sup>N. Komura, K. G. Suzuki, H. Ando, M. Konishi, M. Koikeda, A. Imamura, R. Chadda, T. K. Fujiwara, H. Tsuboi, R. Sheng, *et al.*, *Nat. Chem. Biol* **12**, 402 (2016).